Water hammer modeling by Godunov type finite volume method

S.R. Sabbagh-Yazdi, N.E. Mastorakis, and A. Abbasi

***Abstract*—**In this paper, second-order explicit Finite Volume (FV) Godunov type scheme is applied for water hammer problems and the results are analyzed. The developed one-dimensional model is based on Reimann solution of continuity equation coupled with the momentum equation which includes convective term. The implementation of boundary conditions such as reservoirs, valves, and pipe junctions in the Godunov approach is similar to that of the method of characteristics (MOC) approach. The model is applied to two classic problems (systems consisting of a reservoir, a pipe and a valve). The second-order Godunov scheme is stable for Courant number less than or equal to unity. The minimum and maximum of the computed pressure waves are computed in close agreement with analytical solution and laboratory data.

***Keywords*—**Water-Hammer, Unsteady Pipe Flow, Finite Volume Method, Second Order Godunov Type Reiman Solver

I. Introduction

In pressurized pipeline, flow disturbance caused by pump shutdowns, or rapid changes in valve setting, trigger a series of positive and negative pressure waves large enough to rupture pipelines or damage other hydraulic devices. Negative pressure waves can also result in cavitation, pitting and corrosion. Thus accurate modeling of water hammer events (hydraulic transient) is vital for proper design and safe operation of pressurized pipeline systems. Water quality problems can also arise due to intrusion of contaminants through cracks and joints. Water quality can be affected following a water hammer event as the biofilm on the pipe is sloughed off by large shear stresses created by the transient, and particulates may be resuspended by the strong mixing of the flow inside a pipe. The design of pipeline systems, and the prediction of water quality impacts, requires efficient mathematical models capable of accurately solving water hammer problems.

Various numerical approaches have been introduced for pipeline transient calculation. They include the method of characteristics (MOC), finite difference (FD), wave plan (WP), finite volume (FV), and finite element (FE). Among these methods, MOC proved to be the most popular among water hammer experts. The MOC approach transforms the water hammer partial differential equations into ordinary differential equations along characteristic lines. The integration of these ordinary differential equations from one time step to the next requires that the value of the head and flow at the foot of each characteristic line be known. This requirement can be met by one of two approaches: (i) use the MOC-grid scheme; or (ii) use the fixed-grid MOC scheme and employ interpolation in pipe direction, that it is impossible to make the Courant number exactly equal to one in all pipes. This interpolation artificially modifies the wave celerity and introduces artificial damping into the solution. The fixed-grid MOC is the most widely accepted procedure for solving the water hammer equations and has the attributes of being simple to code, efficient, accurate, and provides the analyst with full control over the grid selection [1].

Results of solving the water hammer equations by the MacCormack, Lambda, and Gabutti explicit FD schemes show that these second-order FD schemes produce better results than the first-order MOC.

Finite element methods (FE) are known for their ability to: (i) use unstructured grids (meshes), (ii) provide fast convergence and accurate results, and (iii) provide results in any point of problem domain. However, the computational work load of the FE solvers motivates the research works on improvement of numerical solvers. For instance, Jovic used the combined method of MOC and FE for water hammer modeling in a classical system (a system consisting of a reservoir, a pipe, and a valve) [2].

FV methods are widely used in the solutions of hyperbolic systems, such as gas dynamics and shallow water waves. FV methods are noted for their ability to: (i) conserve mass and momentum, (ii) provide sharp resolution of discontinuities without spurious oscillations, and (iii) use unstructured grid (mesh). The first order FV method for solution of water hammer problems was highly similar to MOC with linear space-line interpolation [3]. Application of Godunov scheme for the second order FV solution of continuity and momentum equations without convective term produced accurate results for very low Mach numbers [4].

The objective of this article is to apply the Godunov type for FV solution of transient continuity equation coupled with momentum equation without dropping the convective term

Manuscript received June 17, 2007; Revised received October 29, 2007

Saeed-Reza Sabbagh-Yazdi is Associate Professor Civil Engineering Department of K.N. Toosi University of Technology, 1346 Valiasr St. Tehran, IRAN (phone: +9821-88521-644; fax: +9821-8877-9476; e-mail: SYazdi@kntu.ac.ir).

Nikos E. Mastorakis, is Professor of Military Institutes of University Education (ASEI) Hellenic Naval Academy, Terma Chatzikyriakou 18539,Piraues, GREECE (e-mail: mastor@wseas.org).

Ali Abbasi is Graduate Engineering of Civil Engineering Department of K.N. Toosi University of Technology, 1346 Valiasr St. Tehran, IRAN (e-mail: AliAbbasi.civileng@gmail.com).

(which is essential for the cases in which the Mach number is not very low) and investigate the accuracy of the developed method.

The article is organized as follows. First, the governing equations of water hammer are given. Second, the FV form of the governing equations is provided, and then, first- and second-order Godunov schemes for the FV fluxes are formulated. Third, the time integration of the equations is derived. Fourth, the schemes are tested using single pipe systems. Finally, the results are summarized in the conclusion section.

II. Governing Equations

Unsteady closed conduit flow is often represented by a set of 1D hyperbolic partial differential equations [5]:

$$\frac{\partial H}{\partial t}+V\frac{\partial H}{\partial x}+\frac{a^2}{g}\frac{\partial V}{\partial x}+V\sin\theta=0 \tag{1}$$

$$\frac{\partial V}{\partial t}+V\frac{\partial V}{\partial x}+g\frac{\partial H}{\partial x}+J=0 \tag{2}$$

Where, t: time; x:distance along the pipe centerline; $H=H(x,t)$: piezometric head; $V=V(x,t)$: instantaneous average fluid velocity; g: gravitational acceleration; θ : the pipe slope; J: friction force at the pipe wall and a: wave speed defined as,

$$a=\frac{\sqrt{K/\rho}}{\sqrt{1+[(K/E)(D/e)]}} \tag{3}$$

Where, K: bulk modulus of elasticity of the fluid; E: Young's modulus of elasticity for the pipe; ρ : density of the fluid; and e: thickness of the pipe.

The nonlinear convective terms $V\partial H/\partial x$ and $V\partial V/\partial x$ are included in Eqs. (1) and (2). These terms, although small for the majority of water hammer problems, are not neglected in this paper. Maintaining the convective terms in the governing equations makes the scheme applicable to a wide range of transient flow problems.

III. Finite Volume Formulation

The computational grid involves the discretization of the x axis into reaches each of which has a length Δx and the t axis into intervals each of which has a duration Δt. Node (i,n) denotes the point with coordinate $x=[i-(1/2)]\Delta x$ and $t=n\Delta t$. A quantity with a subscript i and a superscript n signifies that this quantity is evaluated at node (i,n).

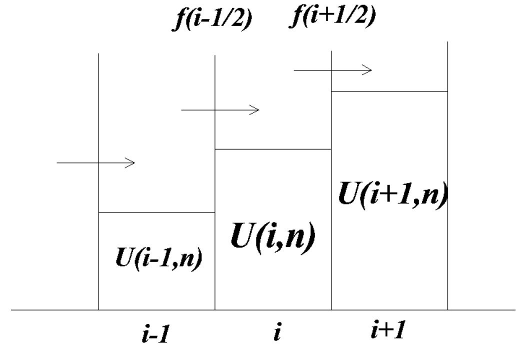

Fig 1. Finite Volume Stencil

The i^{th} control volume is centered at node i and extends from i-$1/2$ to i+$1/2$. That is, the i^{th} control volume is defined by the interval $[(i\text{-}1)\Delta x, i\Delta x]$. The boundary between control volume i and control volume $i+1$ has a coordinate $i\Delta x$ and is referred to either as a control surface or a cell interface. Quantities at a cell interface are identified by subscript such as i-$1/2$ and i+$1/2$ (Fig.1) .

The Riemann-based FV solution of Eqs. (1) and (2) in the i^{th} control volume entails the following steps: (a) the governing equations are rewritten in control volume form; (b) the fluxes at a control surface are approximated using the exact solution of the Riemann problems; and (c) a time integration to advance the solution from n to $n+1$ [6].

Eqs. (1) and (2) can be rewritten in non-conservative form, as,

$$\frac{\partial \boldsymbol{u}}{\partial t}+\frac{\partial \boldsymbol{f}(\boldsymbol{u})}{\partial x}=\boldsymbol{s}(\boldsymbol{u}) \tag{4}$$

where $f(\boldsymbol{u})=\bar{A}\boldsymbol{u}$, $\bar{\boldsymbol{A}}=\begin{pmatrix}\bar{V} & a^2/g\\ g & \bar{V}\end{pmatrix}$ and $\bar{V}$: mean value of V to be specified later. Setting $\bar{V}=0$, the scheme reverts to the classical water hammer case where the convective terms are neglected.

The mass and momentum equations for control volume i is obtained by integration Eq. (4) with respect to x from control surface i-$1/2$ to control surface i+$1/2$. The results is:

$$\frac{d}{dt}\int_{i-1/2}^{i+1/2}\boldsymbol{u}dx+\boldsymbol{f}_{i+1/2}-\boldsymbol{f}_{i-1/2}=\int_{i-1/2}^{i+1/2}\boldsymbol{s}dx \tag{5}$$

Eq. (5) is the statement of laws of mass and momentum conservation for the i^{th} control volume. Let $\boldsymbol{U}_i$ =mean value of u in the interval [i-$1/2$,i+$1/2$]. Eq. (5) becomes

$$\frac{d\boldsymbol{U}}{dt}=\frac{\boldsymbol{f}_{i-1/2}-\boldsymbol{f}_{i+1/2}}{\Delta x}+\frac{1}{\Delta x}\int_{i-1/2}^{i+1/2}\boldsymbol{s}dx \tag{6}$$

The fluxes at cell interfaces can be determined from the Godunov schemes that requires the exact solution of the

Riemann problem. Godunov schemes are conservative, explicit, and efficient. The formulation of a Godunov scheme for the mass and momentum flux $\boldsymbol{f}_{i+1/2}$ in Eq. (6) for all i and for $t \in [t^n, t^{n+1}]$ requires the exact solution of the following Riemann problem:

$$\frac{\partial \boldsymbol{u}}{\partial t} + \frac{\partial \boldsymbol{f}(\boldsymbol{u})}{\partial x} = 0 \qquad (7)$$

where $\boldsymbol{u}^n(x) = \begin{cases} \boldsymbol{U}_L^n & for \quad x < x_{i+1/2} \\ \boldsymbol{U}_R^n & for \quad x > x_{i+1/2} \end{cases}$

where $\boldsymbol{U}_L^n$ = average value of u to the left of interface *i+1/2* at n; and $\boldsymbol{U}_R^n$ = average value of u to the right of interface *i+1/2* at n. The exact solution of Eq. (7) at *i+1/2* for all internal nodes i and for $t \in [t^n, t^{n+1}]$ is as follows:

$$\boldsymbol{u}_{i+1/2}(t) = \begin{pmatrix} H_{i+1/2} \\ V_{i+1/2} \end{pmatrix} = \frac{1}{2}\begin{pmatrix} (H_L^n + H_R^n) + \frac{a}{g}(V_L^n - V_R^n) \\ (V_L^n + V_R^n) + \frac{g}{a}(H_L^n - H_R^n) \end{pmatrix} = \boldsymbol{B}\boldsymbol{U}_L^n + \boldsymbol{C}\boldsymbol{U}_R^n \qquad (8)$$

Where $\boldsymbol{B} = \frac{1}{2}\begin{pmatrix} 1 & a/g \\ g/a & 1 \end{pmatrix}$ and $\boldsymbol{C} = \frac{1}{2}\begin{pmatrix} 1 & -a/g \\ -g/a & 1 \end{pmatrix}$.

Using Eq. (8), the mass and momentum fluxes at i+1/2 for all internal nodes and for $t \in [t^n, t^{n+1}]$ are as follows:

$$\boldsymbol{f}_{i+1/2} = \overline{\boldsymbol{A}}_{i+1/2}\boldsymbol{u}_{i+1/2} = \overline{\boldsymbol{A}}_{i+1/2}\boldsymbol{B}\boldsymbol{U}_L^n + \overline{\boldsymbol{A}}_{i+1/2}\boldsymbol{C}\boldsymbol{U}_R^n \qquad (9)$$

The evaluation of the right-hand side of Eq. (9) requires that $\overline{\boldsymbol{A}}_{i+1/2}$, $\boldsymbol{U}_L^n$, and $\boldsymbol{U}_R^n$ are approximated. To estimate $\overline{\boldsymbol{A}}_{i+1/2}$, the entry associated with the advective terms, $\overline{V}_{i+1/2}$, needs to be approximated. Setting $\overline{V} = 0$ is equivalent to neglecting the advective terms from the governing equations. In general, an arithmetic mean be used to evaluate $\overline{V}_{i+1/2}$.

The explicit evaluation of Eqs. (8) and (9) requires that $\boldsymbol{U}_L^n$ and $\boldsymbol{U}_R^n$ are written in terms of known nodal values.

A. First-Order Godunov Scheme

The first-order Godunov approximation is giving

$$\boldsymbol{U}_R^n = \boldsymbol{U}_{i+1}^n \text{ and } \boldsymbol{U}_L^n = \boldsymbol{U}_i^n \qquad (10)$$

Inserting Eq. (10) into Eq. (9) completes the formulation of the first-order Godunov scheme:

$$\boldsymbol{f}_{i+1/2} = \overline{\boldsymbol{A}}_{i+1/2}\boldsymbol{B}\boldsymbol{U}_i^n + \overline{\boldsymbol{A}}_{i+1/2}\boldsymbol{C}\boldsymbol{U}_{i+1}^n \qquad (11)$$

B. Second-Order Godunov Scheme

In general, the numerical dissipation in first-order scheme is more than in second-order scheme. Limiters increase the order of accuracy of a scheme while ensuring that results are free of spurious oscillations.

Using MINMOD limiter, an approximation for $\boldsymbol{U}_L^n$ and $\boldsymbol{U}_R^n$ that is second order in space and time is obtained by application of following stages at every time step [4]:

At first stage:

$$\boldsymbol{U}_{i-(1/2)^+}^n = \boldsymbol{U}_i^n - 0.5\Delta x MINMOD(\sigma_j^n, \sigma_{j-1}^n) \qquad (12)$$

and

$$\boldsymbol{U}_{i+(1/2)^-}^n = \boldsymbol{U}_i^n + 0.5\Delta x MINMOD(\sigma_j^n, \sigma_{j-1}^n) \qquad (13)$$

where

$$MINMOD(\sigma_j^n, \sigma_{j-1}^n) = \begin{cases} \sigma_j^n & if \quad |\sigma_j^n| < |\sigma_{j-1}^n| \quad and \quad \sigma_j^n.\sigma_{j-1}^n > 0 \\ \sigma_{j-1}^n & if \quad |\sigma_j^n| > |\sigma_{j-1}^n| \quad and \quad \sigma_j^n.\sigma_{j-1}^n > 0 \\ 0 & if \quad \sigma_j^n.\sigma_{j-1}^n < 0 \end{cases} \qquad (14)$$

and

$$\sigma_{j-1}^n = (\boldsymbol{U}_j^n - \boldsymbol{U}_{j-1}^n)/\Delta x \text{ and } \sigma_j^n = (\boldsymbol{U}_{j+1}^n - \boldsymbol{U}_j^n)/\Delta x \qquad (15)$$

At the second stage:

$$\boldsymbol{U}_{i+(1/2)^-}^{n*} = \boldsymbol{U}_{i+(1/2)^-}^n + \frac{1}{2}\frac{\Delta t}{\Delta x}[\boldsymbol{f}(\boldsymbol{U}_{i-(1/2)^+}^n) - \boldsymbol{f}(\boldsymbol{U}_{i+(1/2)^-}^n)] \qquad (16)$$

and

$$\boldsymbol{U}_{i-(1/2)^+}^{n*} = \boldsymbol{U}_{i-(1/2)^+}^n + \frac{1}{2}\frac{\Delta t}{\Delta x}[\boldsymbol{f}(\boldsymbol{U}_{i-(1/2)^+}^n) - \boldsymbol{f}(\boldsymbol{U}_{i+(1/2)^-}^n)] \qquad (17)$$

Finally, the second order scheme is approximated as:

$$\boldsymbol{U}_R^n = \boldsymbol{U}_{i+(1/2)^+}^{n*} \quad \text{and} \quad \boldsymbol{U}_L^n = \boldsymbol{U}_{i+(1/2)^-}^{n*} \qquad (18)$$

Inserting Eq. (18) into Eq. (9) can give Godunov second-order scheme for the solution of Eq.(4).

IV. Boundary Conditions

The implementation of boundary conditions is a important step in solving partial differential equations. The boundary conditions in this model are:

A. Upstream Head-Constant Reservoir

The flux at an upstream boundary (i.e., *i=1/2*) can be determined from the Riemann solution. The Riemann invariant associated with the negative characteristic line is:

$$H_{1/2} - \frac{a}{g}V_{1/2} = H_1^n - \frac{a}{g}V_1^n \quad (19)$$

Coupling this Riemann invariant with a head-flow boundary relation determines:

$$V_{1/2}^{n+1} = V_{1\frac{1}{2}}^n + \frac{g}{a}(H_{1/2} - H_{1\frac{1}{2}}^n) \quad (20)$$

For an upstream reservoir where $H_{1/2}^n = H_{res}$, the flux at the upstream boundary is:

$$\boldsymbol{f}_{1/2} = \begin{bmatrix} \overline{V}_{1/2}H_{res} + \frac{a^2}{g}(V_1^n + \frac{g}{a}(H_{res} - H_1^n)) \\ gH_{res} + \overline{V}_{1/2}(V_1^n + \frac{g}{a}(H_{res} - H_1^n)) \end{bmatrix} \quad (21)$$

B. Fully Closed Downstream valve

The flux at a downstream boundary can be determined from the Riemann solution. The Riemann invariant associated with the positive characteristic line is:

$$H_{Nx+1/2} + \frac{a}{g}V_{Nx+1/2} = H_{Nx}^n + \frac{a}{g}V_{Nx}^n \quad (22)$$

Downstream boundary condition is valve closure in T_c. Head-flow boundary relation determines:

$$V_{Nx+1/2}^{n+1} = V_{steady}(1 - \frac{t}{T_c}) \quad 0 \le t \le T_c \quad (23)$$

$$V_{Nx+1/2}^{n+1} = 0 \qquad t > T_c \quad (24)$$

$$H_{Nx+1/2}^n - H_{Nx-1/2}^n - \frac{a}{g}(V_{Nx+1/2}^{n+1} - V_{Nx-1/2}^n) = 0 \quad (25)$$

As a result, the flux at the boundary is determined as follows:

$$\boldsymbol{f}_{Nx+1/2} = \begin{bmatrix} \overline{V}_{Nx+1/2}(H_{Nx} + \frac{a}{g}V_{Nx}^n - \frac{a}{g}V_{Nx+1/2}) + \frac{a}{g}V_{Nx+1/2} \\ g(H_{Nx} + \frac{a}{g}V_{Nx}^n - \frac{a}{g}V_{Nx+1/2}) + \overline{V}_{Nx+1/2}V_{Nx+1/2} \end{bmatrix} \quad (26)$$

V. Time Integration

The previous section provided a first- and second-order scheme for the flux terms. In order to advance the solution from n to *n+1*, Eq. (6) needs to be integrated with respect to time. In the absence of friction, the time integration is exact and leads to the following:

$$\boldsymbol{U}_i^{n+1} = \boldsymbol{U}_i^n - \frac{\Delta x}{\Delta t}(\boldsymbol{f}_{i+1/2}^n - \boldsymbol{f}_{i-1/2}^n) \quad (27)$$

In the presence of friction, a second order Runge-Kutta solution is used and results in the following explicit procedure:

$$\overline{\boldsymbol{U}}_i^{n+1} = \boldsymbol{U}_i^n - \frac{\Delta x}{\Delta t}(\boldsymbol{f}_{i+1/2}^n - \boldsymbol{f}_{i-1/2}^n) \quad (28)$$

$$\overline{\overline{\boldsymbol{U}}}_i^{n+1} = \overline{\boldsymbol{U}}_i^{n+1} + \frac{\Delta t}{2}\boldsymbol{s}(\overline{\boldsymbol{U}}_i^{n+1}) \quad (29)$$

$$\boldsymbol{U}_i^{n+1} = \overline{\boldsymbol{U}}_i^{n+1} + \Delta t.\boldsymbol{s}(\overline{\overline{\boldsymbol{U}}}_i^{n+1}) \quad (30)$$

The time step should satisfy the Courant-friedrichs-Lewy (CFL) condition for the convective part

$$Cr = \frac{a.\Delta t}{\Delta x} \le 1 \quad (31)$$

Although another stability condition should be used for the updating of a source term, it is found that the CFL condition is sufficient for the cases where the magnitude of the source term is small.

VI. Velocity Dependent Frictions

In this paper, the wall friction is modeled using the following formula [7]:

$$J = \frac{fV|V|}{2D} + k(\frac{\partial V}{\partial t} - a\frac{\partial V}{\partial x}) \quad (32)$$

where D: pipe diameter; f : Darcy- Weisbach friction factor, and k: unsteady friction factor.

VII. Numerical Results

The objective of this section is to compare the accuracy and efficiency of FV solver developed using Godunov scheme in solving transient continuity and equation of motion for water hammer problems. First, the analytical solution and MOC results for a frictionless case are used for assessment of the Cr. Number on the accuracy of the results. Then, the computed results for a case with considerable pipe roughness are compared with laboratory measurements.

A. Test Case I

This test case consists of a simple reservoir-pipe-valve configuration. The geometrical and hydraulic parameters for this frictionless test case are given in Table 1.

Table 1. Geometrical and hydraulic parameters for test case I

Pipe diameter (m)	0.5
Pipe length (m)	1000
D.W friction factor	0.00
Unsteady friction factor	0.00
Wave speed(m/s)	1000
Reservoir head-upstream (m)	0
Initial mean velocity(m/s)	1.02
Cause of transients	Downstream instantaneous fully valve closure

This problem is solved by previous workers using a Godunov scheme for solving the continuity equation and momentum equation in which the convective term is omitted [4].

Analytical solution [4] and [8], and MOC results [1] and [9] are used to investigate the accuracy of proposed model which uses Godunov scheme for FV solution of the continuity equation coupled with momentum equation which includes the convective term.

Figure 2 shows the comparison of the results computed by present FV method with analytical solutions and results of MOC for the variations in hydraulic head at the valve as a function of time. As expected, the head traces results by both schemes (MOC and FVM) exhibit numerical dissipation for Cr=0.1, but the numerical dissipation in FVM is considerably less than the MOC. It worth noting that, the finite volume solution using Godunov scheme corresponds to the analytical solution when Cr=1.0. But for Courant number less than one, the minor numerical dissipations appear in the solution results (Fig.3).

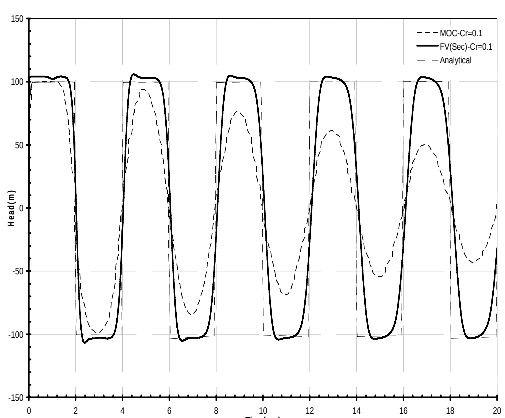

Fig 2. Variations in hydraulic head at the valve (Test I) for MOC, FVM and analytical solution

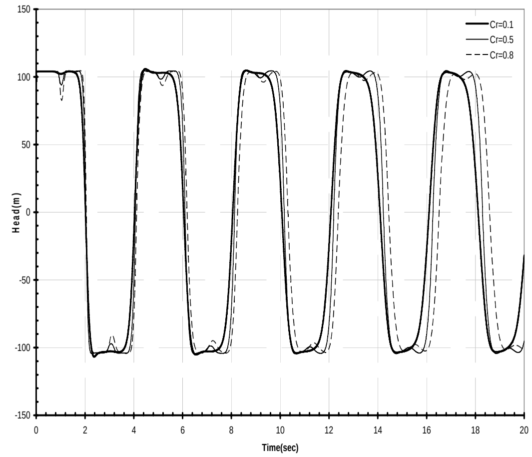

Fig 3. Pressure head traces at valve (Test I) for various Cr No.(FVM)

B. *Test Case II*

In this test case, laboratory data [10] for a sudden closure of a valve downstream of a pipe with wall roughness are used to investigate the accuracy of the FV scheme. The geometric, kinematics, and dynamic parameters of this test are summarized in Table 2.

Table 2. Properties for the test case 2

Pipe diameter (m)	0.022
Pipe length (m)	37.20
D.W friction factor	0.034
Unsteady friction factor	0.00
Wave speed(m/s)	1319
Reservoir head-upstream (m)	32.0
Discharge(Lit/s)	0.114
Density(kg/m^3)	1000
Viscosity(m^2/s)	1.02
Cause of transients	Downstream valve closure in 0.009 seconds

In figure 4 the results of present FV and MOC solvers and are compared with laboratory measurements. As can be seen in figure 4, although the time period of the pressure waves are computed reasonably by both numerical models, the finite volume scheme produce much better pressure values distribution than the MOC.

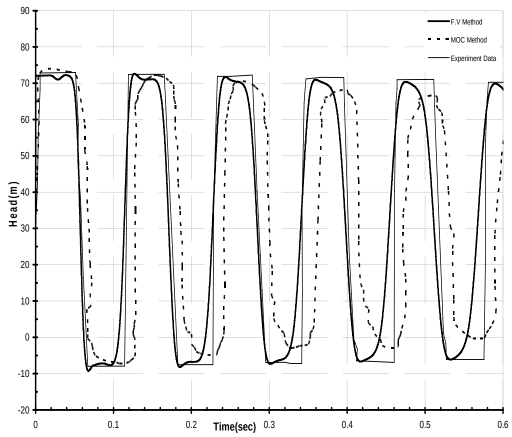

Fig 4. Variations in hydraulic head at the valve (Test II) for MOC and FVM and laboratory data (Cr=0.5)

VIII. CONCLUSION

In this paper, second-order explicit Godunov-type finite volume scheme for coupled solution of transient continuity equation and momentum equation (with convective term) is formulated and applied for numerical investigations. The results of present FV solver are compared with numerical data produced by a MOC model, analytical solution (for frictionless case) as well as measured data reported by other researchers (for rough pipe). The results of present investigations are as follows.

-Inclusion of the nonlinear convective terms to the mathematical equations does not disturb the results of solution water hammer problems by present model.

- The maximum and minimum of the pressure waves computed by FVM are in close agreements with analytical and experimental data.

- Numerical dissipation in Godunov-type FV method is less than MOC, and therefore, the Godunov-type FV solver produces considerably more accurate than the MOC for a Courant number less than or equal to one.

The present Godunov-type FV solver can be used for the transient pipe flow problems in which the convection effect is not neglegible.

REFERENCES

[1] M. S. Ghidaoui and B. W. Karney, *Equivalent Differential Equations in Fixed-Grid Characteristics Methods*, J. Hydraul. Eng., 120(10) , (1994, pp 1159-1175.

[2] V. Jovic, *Finite Element and Method of characteristics Applied to water Hammer Modeling*, Int. J. for Engng. Modeling, 8(3&4), 1995, pp 21-28.

[3] V. Guinot, *Riemann Solvers for Water-Hammer Simulations by Godunov Method*, Int. J. Numer. Meth. Eng, 49, 2000, pp 851-870.

[4] M. Zhao and M. S. Ghidaoui, *Godunov-Type Solution for Water Hammer Flows*, J. of Hydraul. Engng, 130(4), 2004, pp 341-348.

[5] E. B. Wylie and V. L. Streeter,. *Fluid Transients in System*. Prentice-Hall, Engle-wood, 1993.

[6] E. F. Toro, *Reimann Solvers and Numerical Methods for Fluid Dynamics*, Springer, Berlin, 1997.

[7] G. Brunone, B. W. Karney, M. Mecarelli.and M.Ferrante, *Velocity Profiles and Unsteady Pipe Friction in transient Flow*, J.. Water Resource Planing and Management.,126(4), 2000, pp 236-244.

[8] B. B. Sharp, *Water-Hammer Problems and Solutions*, University Of Melborn Edward Arnold Ltd, 1981.

[9] M. Turani, *MOC Water Hammer Analysis of Karoun IV Dam Hydropower Penstocks*, M.Sc Thesis in Civil Engineering, K.N.T. University of Technology, Tehran, Iran, 2003 (Farsi).

[10] A. Bergant and A. R. Simpson, Estimating Unsteady Friction in Transient Cavitating Pipe Flow, Proceeding of 2nd Int. Conf. on Water Pipe Line Systems, Edinbrugh, UK , 24-26 May 1994, Conf. Series Publ. 110, 3-15.

First Author's biography may be found in following site:
http://sahand.kntu.ac.ir/~syazdi/